

# Charge-transport model for conducting polymers

Stephen Dongmin Kang<sup>1,2</sup> and G. Jeffrey Snyder<sup>1,2\*</sup>

The growing technological importance of conducting polymers makes the fundamental understanding of their charge transport extremely important for materials and process design. Various hopping and mobility edge transport mechanisms have been proposed, but their experimental verification is limited to poor conductors. Now that advanced organic and polymer semiconductors have shown high conductivity approaching that of metals, the transport mechanism should be discernible by modelling the transport like a semiconductor with a transport edge and a transport parameter  $s$ . Here we analyse the electrical conductivity and Seebeck coefficient together and determine that most polymers (except possibly PEDOT:tosylate) have  $s = 3$  and thermally activated conductivity, whereas  $s = 1$  and itinerant conductivity is typically found in crystalline semiconductors and metals. The different transport in polymers may result from the percolation of charge carriers from conducting ordered regions through poorly conducting disordered regions, consistent with what has been expected from structural studies.

Organic semiconductors provide a unique processing advantage<sup>1,2</sup> over inorganic materials, putting them in a strong position for innovative electronic applications. Organic light-emitting diodes are already part of the mainstream technology in displays and the advances in organic field-effect transistors (FETs) are further driving the technology towards flexible displays<sup>3</sup>. Flexible photovoltaics enabled by the use of conducting polymer layers have now reached competitive efficiencies<sup>4–6</sup>. Some polymers have promising properties for thermoelectric applications<sup>7,8</sup>, increasing interest in thermopower measurements.

Progress in semiconducting polymers has led to carrier mobilities exceeding that of amorphous silicon<sup>9–11</sup>, with a focus on controlling and understanding the structural aspects<sup>12,13</sup>. Nevertheless, one of the foremost and persistent challenges in the burgeoning field of polymer electronics and thermoelectrics is the fact that there is no robust transport model<sup>12,14</sup> to guide further development in these complex systems.

In crystalline semiconductors and metals the free-electron approximation for the band structure enables the effective use of a mobility  $\mu$  and free-carrier concentration  $n$  to describe the electrical conductivity  $\sigma = |e|n\mu$ . In disordered polymers there are many localized charge carriers by which charge transport is often described by hopping from site to site. It then may become a challenge to clearly define a free-carrier concentration and mobility. Here we will avoid this complication and analyse the conductivity in a much generalized form applicable to all mechanisms of electronic conduction: from metals to hopping insulators.

## Generalized charge-transport model

Most charge-transport theories can be described by generalized Boltzmann transport equations (see Methods and Supplementary Information) where electrical conductivity  $\sigma$  can be characterized by the transport function  $\sigma_E(E)$ :

$$\sigma = \int \sigma_E \left( -\frac{\partial f}{\partial E} \right) dE \quad (1)$$

$\sigma_E(E)$  has units of conductivity but is the measured conductivity only when all mobile carriers have the same energy (for example, at the electron chemical potential ( $E_F$ ) in a metal at low  $T$ ). In general, the measured conductivity  $\sigma$  will sample the

transport function  $\sigma_E(E)$  in an energy width of  $\approx 4k_B T$  around  $E_F$ . This is because electrons are fermions that must also have an unoccupied state accessible to transport, leading to the function  $-\partial f / \partial E = f(1-f)/k_B T$  (where  $f$  is the Fermi-Dirac distribution function) in equation (1) to select only the mobile electrons from  $\sigma_E(E)$  to get the true conductivity  $\sigma$ .

The form of  $\sigma_E(E)$  that we find fits the transport data for a wide range of semiconducting polymers over the entire measurable range of conductivity has two essential features that will help identify the transport mechanism: a transport edge  $E_t$  and transport parameter  $s$ .

$$\begin{aligned} \sigma_E(E, T) &= \sigma_{E_0}(T) \times \left( \frac{E - E_t}{k_B T} \right)^s & (E > E_t) \\ &= 0 & (E < E_t) \end{aligned} \quad (2)$$

where  $E/k_B T$  is the reduced energy of the charge carriers (electrons or holes) and  $\sigma_{E_0}(T)$  is a temperature-dependent but energy-independent parameter, which we call the transport coefficient. The existence of a transport edge is essential for describing the nearly insulating polymers with  $E_F \ll E_t$ , while semiconductors with  $E_F$  near  $E_t$  are further characterized by the energy dependence above the edge using the transport parameter  $s$  as an exponent.

Like a band edge, the transport edge is the transport energy  $E_t$  of charge carriers below which no electrons or holes exist or have no contribution to conductivity even at finite temperature (Fig. 1a). In a crystalline semiconductor or insulator there are no charge carriers with energy  $E < E_t$ , so the transport edge is the band edge. Carriers with energy below the transport edge must be thermally excited to an energy above the transport edge to conduct electricity (this is accounted for in the distribution function  $f$  in equation (1)).

Here we define the transport edge to be when  $\sigma_E(E)$  becomes nonzero at finite temperature. More often the term mobility edge is used, originally to describe homogeneously disordered systems, where the mobility edge is defined when  $\sigma_E(E)$  and mobility become nonzero at  $T = 0$  K, which happens when the electronic states are fully delocalized across the sample as is considered for a true metal<sup>15</sup>. Charge carriers with energy above the mobility edge are itinerant and freely conduct electricity like a metal. The transport edge we find here from measurements in doping studies is fundamentally different from a mobility edge because the conductivity is thermally

<sup>1</sup>Department of Applied Physics and Materials Science, California Institute of Technology, California 91125, USA. <sup>2</sup>Department of Materials Science and Engineering, Northwestern University, Illinois 60208, USA. \*e-mail: jeff.snyder@northwestern.edu

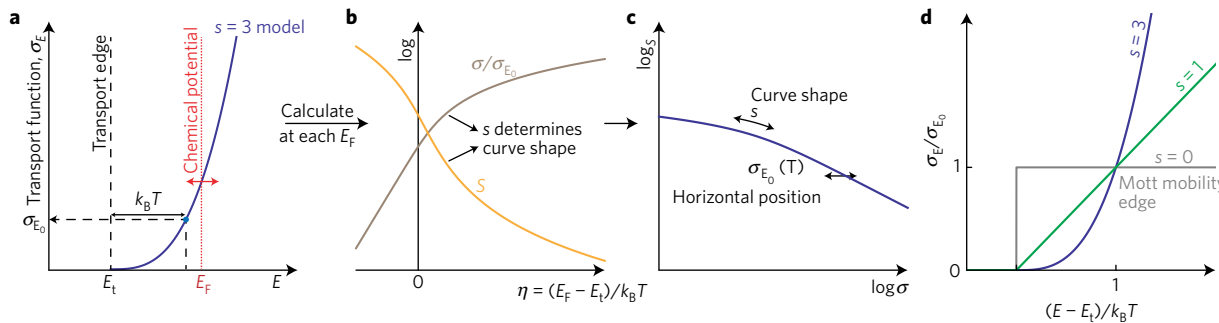


**Figure 1 | Schematic of the  $\sigma_E$  transport model and analysis procedure.** **a**, The transport function  $\sigma_E(E)$  for the  $s=3$  model (equation (2)). The transport coefficient  $\sigma_{E_0}(T)$  is the value at a reference point ( $E=E_t+k_B T$ ). The transport function in the proximity of the chemical potential ( $E_F$ ) governs the transport properties. **b**, The measured electrical conductivity (normalized by  $\sigma_{E_0}$ ) and Seebeck coefficient will depend on the reduced chemical potential  $\eta=(E_F-E_t)/k_B T$  as described with the model curve (see Methods). The curve shape depends only on the transport parameter  $s$ . **c**, The Seebeck coefficient versus conductivity relation obtained by eliminating the parameter  $\eta$  in **b**. The curve has only two fitting parameters:  $s$  determines the curve shape and the transport coefficient  $\sigma_{E_0}(T)$  determines the magnitude of the conductivity. **d**, Comparison of different transport functions. Mott's mobility edge model corresponds to  $s=0$ .

activated (such as hopping transport) even for carriers with energy above the transport edge.

The conductivity of a non-crystalline material is often described with an Arrhenius equation of the form  $\sigma(T) \propto \exp(-E_a/k_B T)$ , where  $\sigma(T)$  is the experimental conductivity<sup>16</sup>. In the Supplementary Information we show that this Arrhenius activation energy ( $E_a$ ) can arise from both  $E_F$  being below the transport edge  $E_t$  as well as any sort of activation energy  $W$  that may involve hopping. It is difficult to distinguish these two energies ( $E_t - E_F$  and  $W$ ) with conductivity alone, thus requiring an independent measurement, such as thermopower, to identify a transport mechanism. Using the thermopower (Seebeck coefficient) to account for  $E_t - E_F$ , we can uniquely determine  $W$  and ultimately clues to the percolation conduction mechanism in conducting polymers as depicted schematically in Fig. 2.

Charge carriers that can be induced to migrate by an electric field can also be so induced by a temperature gradient, which can be characterized by the Seebeck coefficient (or thermopower for its magnitude). While each charge carrier has a charge  $e$  with it, it also carries an ‘excess’ energy  $E - E_F$ . The Seebeck coefficient can also be simply described by the transport function  $\sigma_E(E)$  accounting for the energy of each carrier rather than the charge:

$$S = \frac{1}{\sigma} \left( \frac{k_B}{e} \right) \int \left( \frac{E - E_F}{k_B T} \right) \sigma_E \left( -\frac{\partial f}{\partial E} \right) dE \quad (3)$$

The Seebeck coefficient in insulators or hopping conductors is commonly approximated as  $S = (E_t - E_F)/eT$  or its reformulation as the Heikes formula (see Supplementary Information for derivation using  $\sigma_E$ ); this form demonstrates that  $S$  is sensitive to  $E_t - E_F$  but independent of  $W$ . Because the Seebeck coefficient is an independent measurement of the same general transport function  $\sigma_E$  as for electrical conductivity, measuring both properties on the same samples enables the determination of the transport mechanism, particularly once  $E_F$  has reached the vicinity of  $E_t$ .

Once above the transport edge, different transport mechanisms predict different forms for  $\sigma_E(E)$ . Different conduction mechanisms have fundamentally different energy dependencies because  $\sigma_E(E)$  generally depends on the density of states, charge carrier velocity, and their relaxation time or hopping frequency. Each of these typically has a power-law relationship to the energy of the carrier above the transport edge. Thus, a general form for  $\sigma_E(E)$  is a power law with  $s$  in equation (2) (Fig. 1d). This form is used to calculate  $S$  versus  $\sigma$  relations (Fig. 1a–c) that can be used to identify the parameter  $s$  and connect to transport mechanisms.

### Transport model for conducting polymers

By compiling extensive polymer doping studies from the literature, universal trends are found in a plot of  $S$  versus  $\sigma$  (Fig. 3a,b); however, these are not explainable by either of the two models, both pioneered by Mott<sup>15</sup>, that are most used to describe conducting polymers<sup>17,18</sup>. The variable range hopping model, which describes hopping processes between localized states, generally yields a small thermopower on the order of  $10 \mu\text{V K}^{-1}$ , whereas thermopower observed in polymer semiconductors easily exceeds such low estimates. Mott’s mobility edge model is used to describe metallic-like transport for carriers excited above a transport edge (that is also a mobility edge because the charge carriers are thought to have free-electron-like properties). The fact that experimentally measured conductivity is always unlike a metal, being thermally activated in polymers, is an obvious failure of the model. Moreover, as has been pointed out in ref. 14, both of Mott’s models predict a thermopower–conductivity relation that is qualitatively different from experimental observations (see the mobility edge ( $s=0$ ) and variable range hopping model evaluations in Fig. 3a). Instead of a mechanistic model, the universal trend<sup>14,17,19</sup> in  $S$  versus  $\sigma$  has been fit empirically to  $S \propto \sigma^{-1/4}$  in ref. 14.

Despite the failure of the hopping and mobility edge models, a simple form of the transport function (equation (2)) is all that is required to successfully model the data with two simple parameters:  $s$  and  $\sigma_{E_0}(T)$ . The transport edge  $E_t$  that sets the onset of conduction, which is required to model the thermopower and conductivity of insulating samples, is like a mobility edge but without requiring metal-like transport above the edge. The energy dependence of  $\sigma_E(E)$  described with a transport exponent  $s$  is a common form found in metals and semiconductors that characterizes the general conduction mechanism (including density of states and scattering).  $\sigma_{E_0}(T)$  plays the role of mobility, which will become essential when mobility is hard to measure or even define.

The  $S$  versus  $\sigma$  curve, spanning eight orders of magnitude of conductivity, can be fitted with equation (2) using  $s=3$ , revealing an identical transport exponent for these typical conducting polymers. In three-dimensional crystalline solids,  $s=1$  is typical but  $s=3$  can be expected when charge carriers are scattered by ionized impurities<sup>20</sup>. Although this resemblance could be attributed to the charge-transfer nature of doping in polymer semiconductors, the Arrhenius-like temperature dependence of polymer semiconductors suggests that such a model for metallic extended states may not be applicable.

The value of  $\sigma_{E_0}(T)$  determines the magnitude of the conductivity, functioning as a weighted mobility. The values

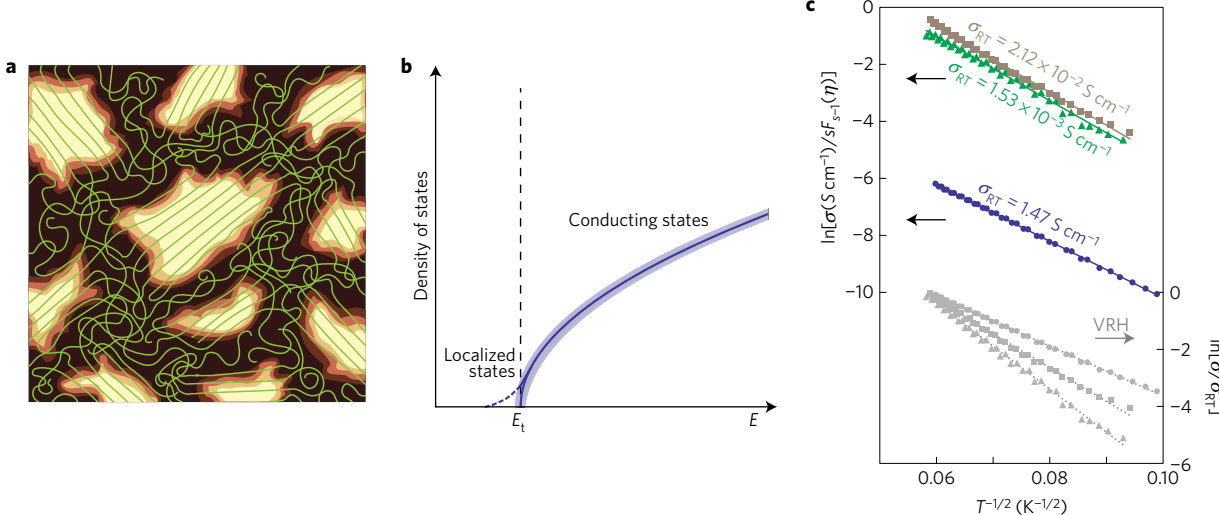


**Figure 2 | Percolation transport in polymers.** **a**, Schematic of the inhomogeneous disorder<sup>23</sup> based on microstructure studies<sup>12,24</sup>. The background colour illustrates local conductivity, where brighter regions are more conductive<sup>24,32</sup>. The connection between the conductive ordered domains (percolation path) limits  $\sigma_{E_0}$  (and thus the magnitude of the conductivity), causing thermally activated conduction. **b**, Density of states. States below the transport edge  $E_t$  are truly localized and do not contribute to conduction. States above  $E_t$  conduct electricity, but this involves thermally activated conduction. **c**, Temperature-dependent transport coefficient  $\sigma_{E_0}$  of polyacetylene analysed using the  $s=3$  model. Data points are by analysing three sets of paired thermopower and electrical conductivity data from ref. 22.  $\eta(T)$  is obtained from  $S(T)$ , by which  $\sigma(T)$  is scaled to obtain  $\sigma_{E_0}(T)$ . Solid lines are from fitting to equation (4) with  $\gamma=1/2$ , where the slope determines the activation energy  $W_\gamma$ . The three samples yield an average of  $W_{1/2}=1.0 \pm 0.1$  eV. For comparison, analysis using the variable range hopping model is shown (grey data points and dotted lines), where each sample yields a different hopping energy. The room-temperature conductivity of each sample is indicated in the figure.

of  $\sigma_{E_0}(T=300\text{ K})$ , like mobilities measured in a FET<sup>9</sup>, show a stronger correlation with the preparation rather than with a specific material. In principle, inducing mobile charge carriers electrostatically in a material like done in an FET, adjusts the  $E_F$  and could enable a more direct measurement of  $\sigma_E(E)$  without the need of the Seebeck measurement. However, the mobility  $\mu$ , as defined through the Drude free-electron model  $\sigma=|e|n\mu$ , necessitates the knowledge of free-carrier concentration  $n$  to relate to conductivity  $\sigma$ . In most polymer conductors, it may not be obvious which carriers to count in  $n$ .

Because the form of  $\sigma_E(E)$  in equation (2) is rather general, being unbiased regarding mechanisms, it can help with the debate over the role of hopping versus extended states in polymer conductors<sup>18</sup>. Recall that the temperature-activated conductivity observed in polymer semiconductors, even at metallic doping levels, is a distinct characteristic of conducting polymers. Our model analysis allows us, by using the information from the thermopower, to refine the method of how activation energies are obtained. We apply this approach to polyacetylene to argue that the extracted activation energies are not necessarily related to hopping conduction between Anderson-localized states<sup>17</sup>.

### Percolation in conducting polymers

It is common practice to extract activation energies by plotting  $\ln\sigma$  against  $T^{-\gamma}$ , with  $\gamma$  depending on the interpretation of hopping<sup>15,17</sup>. A fit to such a power law is sometimes considered a signature of hopping between localized states. However, this approach gives an activation energy that is inseparable from any dependencies on the chemical potential. Similar aspects have been pointed out in a study on amorphous Si<sup>21</sup>.

Instead, with  $S(T)$  and  $\sigma(T)$  from the same sample, one can obtain the reduced chemical potential  $\eta(T)=(E_F-E_t)/k_B T$  by using the  $\sigma_E$  of equation (2) with equation (3) (that is, equation (8)), and then extract  $\sigma_{E_0}(T)$  from which an activation energy can be fitted (Fig. 2c and Supplementary Fig. 7). By using data of polyacetylene reported in ref. 22, we analyse the

temperature-dependent transport coefficient  $\sigma_{E_0}(T)$  based on a form commonly used for analysing polymers:

$$\sigma_{E_0} \propto \exp \left[ - \left( \frac{W_\gamma}{k_B T} \right)^\gamma \right] \quad (4)$$

where the energy  $W_\gamma$  depends on the choice of  $\gamma$ . Following the most widely used choice of  $\gamma=1/2$  for polymers, we obtain the same  $W_{1/2}=1.0 \pm 0.1$  eV for three different polyacetylene samples with vastly different conductivities ranging three orders of magnitude, as shown through the identical slopes in Fig. 2c. By contrast, the variable range hopping expression ( $\ln\sigma \propto T^{-\gamma}$ ) yields an activation energy that varies almost twofold, as also shown in Fig. 2c. Finding a constant  $W_{1/2}$  value suggests our approach is revealing a fundamental aspect of the transport mechanism. The traditional description using a mobility edge (rather than a transport edge) is not applicable here because the identical activation energy still exists when the chemical potential is above ( $\eta>0$ ) as well as below ( $\eta<0$ ) the edge (Supplementary Fig. 7a). Therefore, the activation energy observed in polyacetylene should be explained with a different picture.

The inhomogeneous disorder in polymer semiconductors<sup>12,23,24</sup> (Fig. 2a) leads us to consider the subpercolation limit (transport being limited by the connectivity of conducting ordered domains because of the presence of poorly conducting disordered domains acting as an energy barrier) as a cause for the temperature dependency of conductivity, which is in contrast to Mott's model that assumes sample homogeneity<sup>15</sup>. Percolation studies with metal crystallites in dielectric media<sup>25</sup> have shown cases of percolation conduction that exhibit an activated behaviour that resembles Mott's variable range hopping model despite being a different physical picture. The energy dependence of  $\sigma_E(E)$  in a percolation system could also scale with energy in a power law<sup>15,26</sup>, contributing to the transport parameter  $s$ . The percolation contribution to  $s$  will combine with that from the ordered domains that could be distinguished through local transport property measurements.

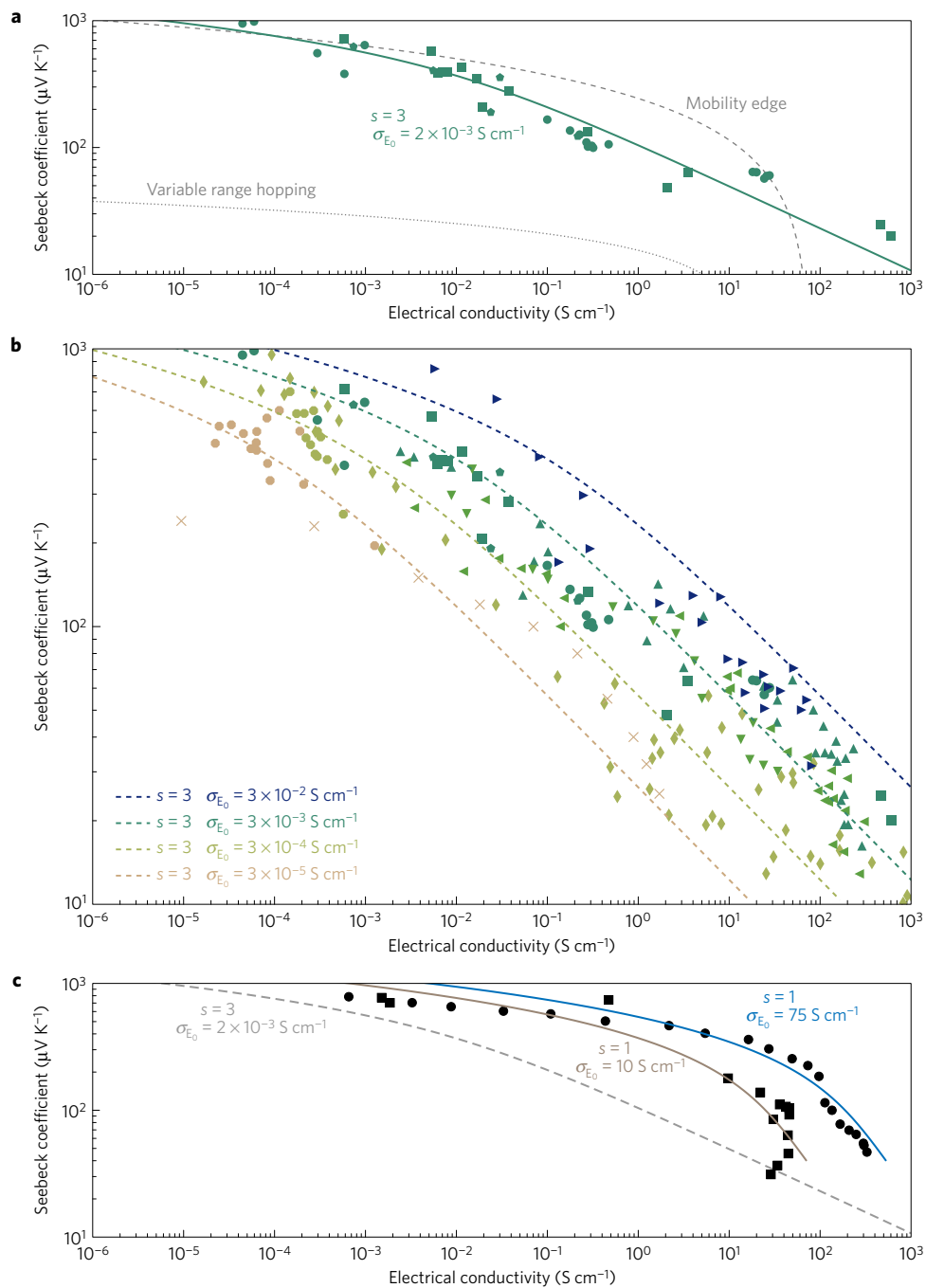


**Figure 3 | The thermopower versus electrical conductivity relation at room temperature, comparing various models.** **a**, The solid line was calculated using the parameters given in the figure. Plotted together are data from ref. 14, including: P3HT (green circle); PBTET-C<sub>14</sub> (green square); P2TDC<sub>17</sub>-FT4 (green pentagon). The samples were doped with either F4TCNQ or FTS. The relations given by the variable range hopping model (grey dotted line) and Mott's mobility edge model (grey dashed line), as evaluated in ref. 14, are plotted together for comparison. **b**, Compilation of literature data showing the range of  $\sigma_{E_0}$  values found in polymer semiconductors. The dashed lines are obtained with the  $s = 3$  model. As a guide to eyes, the symbols are coloured in accordance to the approximate value of average  $\sigma_{E_0}$  observed in each data set. Additional data points represent: PDPP3T (filled blue right-triangle), P3HT (filled green up-triangle), PBTET (filled green left-triangle), PSBTBT (filled green down-triangle) from ref. 33; polyacetylene (filled green lozenge) as compiled in ref. 17; P3HT:F4TCNQ mixed P3HTT (filled green octagon, filled peach octagon) from ref. 34; P3HT (peach cross mark) from ref. 35. Chemical abbreviations are given in the Supplementary Information. **c**, The thermopower versus electrical conductivity relation of PEDOT:tosylate (filled black circle) from ref. 7 and PEDOS-C<sub>6</sub> (filled black square) from ref. 28, modelled with  $s = 1$ . Shown together is the model calculation for the  $s = 3$  case shown in **a**. It is seen that the curves are qualitatively different, and also that  $\sigma_{E_0}$  is orders of magnitude higher in the case of the samples shown.

The percolation mechanism for charge transport is consistent with recent microstructural investigations. By analysing the electroluminescence spectra of P3HT films, it was concluded in ref. 12 that charge transport occurs through the ordered

regions (aggregates—ordering by  $\pi$  stacking) that exist within an inhomogeneously disordered matrix. In another study<sup>27</sup>, it was shown that FET mobility increases by orders of magnitude with a small increase in the volume fraction of aggregates indicating

subpercolation behaviour. In such a regime, the transport between ordered domains limits  $\sigma_{E_0}(T)$ ; improving the structural connectivity of ordered domains has been shown as one way to improve the percolation for transport<sup>12,27</sup>. The trapping mechanism by localized states<sup>18</sup> located within the ordered domains<sup>12</sup> as a cause for the thermally activated behaviour<sup>12</sup> is not supported by our analysis of polyacetylene. In such a trapping limited case,  $W_\gamma$  should diminish as the chemical potential reaches above the transport edge (which is also the mobility edge in the trapping model).

Microstructural effects on the percolation will be reflected through the  $\gamma$  and  $W_\gamma$  terms. Improved film morphologies are expected to reduce  $W_\gamma$ , which is related to the energy barrier for transport between the ordered regions. A change in  $\gamma$  indicates that the factors that determine the optimal conduction path, such as dimensionality or connectivity of domains, have changed. For example, the transition associated with the inter-aggregate distance approaching the persistence length of tie molecules<sup>27</sup> is expected to cause a change in  $\gamma$ .

### Exceptional transport in PEDOT

Remarkably high conductivity has been reported for poly(3,4-ethylenedioxythiophene) (PEDOT)-based materials leading to considerable interest in applications such as thermoelectrics<sup>7,28</sup>. We find that these high-performance PEDOT-based samples are fundamentally different giving a better fit to the  $S - \sigma$  curve by  $s = 1$  than  $s = 3$  of other polymers (Fig. 3c). The  $\sigma_{E_0}$  extracted from the fit is a few orders of magnitude higher than the majority of polymers that follow  $s = 3$ , resulting in higher conductivity for a given thermopower.

The different  $s$  parameter could be understood as a different ‘type’ of charge transport, which might be associated with the unusual behaviour found in similar materials<sup>29</sup>. Although the mathematical form of equation (2) suggests that a transport type with higher  $s$  would be beneficial for conduction, it seems that  $s = 1$  tends to provide a higher  $\sigma_{E_0}$ . Analogous situations are found in inorganic semiconductors where acoustic-phonon scattering ( $s = 1$ ) generally results in a higher mobility than ionized-impurity scattering ( $s = 3$ )<sup>20</sup>. We tentatively anticipate that searching for cases with  $s = 1$  could lead to the discovery of high- $\sigma_{E_0}$  polymers.

We note that the transport edge described in the model probably describes an effective global transport edge of the sample. Locally, there may be a distribution of transport and mobility edges at different energies that would presumably depend on the degree of disorder. Energetic disorder of the mobility edge in the form of a Gaussian distribution is not expected to have a significant impact on  $s$ ; convolution of a form  $x^s$  with a Gaussian preserves the exponent  $s$ .

### Estimating maximum thermoelectric performance

Our analysis provides a means to estimate the maximum thermoelectric performance that can be obtained from a given material. The thermoelectric figure of merit ( $zT$ ) is a function of both the material quality and the chemical potential (doping level). As long as the material is fixed (with a fixed  $\sigma_{E_0}$ ), the maximum achievable  $zT$  through doping optimization is also bounded, as illustrated in Fig. 4.

Such an estimation of a material is readily done using the thermoelectric material quality factor<sup>30</sup> that is determined by  $\sigma_{E_0}$  and  $\kappa_l$ , the lattice portion of thermal conductivity:

$$B = \left( \frac{k_B}{e} \right)^2 \frac{\sigma_{E_0} T}{\kappa_l} \quad (5)$$

Each solid line in Fig. 4 represents a fixed  $B$ , where the maximum  $zT$  can be predicted simply from the value of  $B$  (as described in the Supplementary Information) that is determined primarily

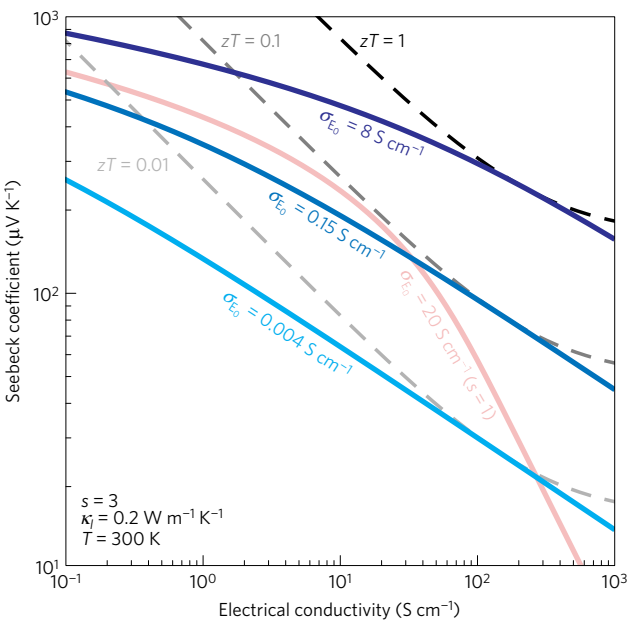


**Figure 4 | Contour plot (dashed lines) of thermoelectric figure of merit  $zT$  (assuming  $\kappa_l = 0.2 \text{ W m}^{-1} \text{ K}^{-1}$  and  $T = 300 \text{ K}$ ).** Coloured solid lines each represent a family of conducting polymers (that is, same  $\sigma_{E_0}$ ) with different doping (such behaviour upon doping was found experimentally in Fig. 3). The optimum doping (intersecting point of the solid and dashed lines) is typically found in materials with electrical conductivity between  $10^1$  and  $10^3 \text{ S cm}^{-1}$ . For example, with doping adjusted for conductivity of  $100 \text{ S cm}^{-1}$ , thermopower around  $100 \mu\text{V K}^{-1}$  (corresponding to  $\sigma_{E_0} = 0.15 \text{ S cm}^{-1}$ ) is required to achieve  $zT = 0.1$ . The curves for a different mechanism (for example,  $s = 1$ , red solid line) require similar magnitude of thermopower and conductivity for the same  $zT$  (although the  $\sigma_{E_0}$  will be very different).

by the transport coefficient  $\sigma_{E_0}$  (equation (5)). Assuming polymer conductors can achieve  $\kappa_l = 0.2 \text{ W m}^{-1} \text{ K}^{-1}$ , the best  $s = 3$  conducting polymers of Fig. 3b with  $\sigma_{E_0} \leq 0.003 \text{ S cm}^{-1}$  should have maximum  $zT \leq 0.01$  at 300 K. To achieve  $zT > 0.1$ , much higher values of  $\sigma_{E_0}$ , as reported for PEDOT:Tos with an atypical mechanism ( $s = 1$ ), is required.

In summary, the temperature-dependent data pairs of  $S(T)$  and  $\sigma(T)$  analysed with the transport function  $\sigma_E(E)$  prompt a rethinking of the nature of conduction in semiconducting polymers. We emphasize that unsuccessful explanation for the thermopower-conductivity relation is not merely a failure in describing thermopower, but is a failure in the charge-transport model itself. We uncover the  $s = 3$  model for  $\sigma_E(E)$  and unique temperature dependence of polymers (thermally activated conductivity above  $E_t$ ) and attribute it to inhomogeneous disorder found in structural studies. Further investigation utilizing pairs of  $S(T)$  and  $\sigma(T)$  (both locally and macroscopically) and other perhaps more direct measurements of  $\sigma_E(E)$  on complex materials—not just polymers but any disordered and/or inhomogeneous materials with microstructure at multiple length scales<sup>31</sup>—could provide insight regarding microstructure, disorder and percolation.

### Methods

Methods and any associated references are available in the online version of the paper.

Received 10 March 2016; accepted 19 September 2016;  
published online 14 November 2016

## References

1. LeBlanc, S., Yee, S. K., Scullin, M. L., Dames, C. & Goodson, K. E. Material and manufacturing cost considerations for thermoelectrics. *Renew. Sustain. Energy Rev.* **32**, 313–327 (2014).
2. Yee, S. K. *Thermoelectric Generators: a Material, Device, and Cost Perspective* (2015 MRS Fall Meeting, 2015).
3. Sirringhaus, H. 25th anniversary article: organic field-effect transistors: the path beyond amorphous silicon. *Adv. Mater.* **26**, 1319–1335 (2014).
4. Service, R. F. Outlook brightens for plastic solar cells. *Science* **332**, 293 (2011).
5. Green, M. A., Emery, K., Hishikawa, Y., Warta, W. & Dunlop, E. D. Solar cell efficiency tables (Version 45). *Prog. Photovolt. Res. Appl.* **23**, 1–9 (2015).
6. Malinkiewicz, O. *et al.* Perovskite solar cells employing organic charge-transport layers. *Nat. Photon.* **8**, 128–132 (2014).
7. Bubnova, O. *et al.* Optimization of the thermoelectric figure of merit in the conducting polymer poly(3,4-ethylenedioxythiophene). *Nat. Mater.* **10**, 429–433 (2011).
8. Kim, G. H., Shao, L., Zhang, K. & Pipe, K. P. Engineered doping of organic semiconductors for enhanced thermoelectric efficiency. *Nat. Mater.* **12**, 719–723 (2013).
9. Kang, K. *et al.* 2D coherent charge transport in highly ordered conducting polymers doped by solid state diffusion. *Nat. Mater.* (2016).
10. Venkateshvaran, D. *et al.* Approaching disorder-free transport in high-mobility conjugated polymers. *Nature* **515**, 384–388 (2014).
11. Zhang, X. *et al.* Molecular origin of high field-effect mobility in an indacenodithiophene-benzothiadiazole copolymer. *Nat. Commun.* **4**, 2238 (2013).
12. Noriega, R. *et al.* A general relationship between disorder, aggregation and charge transport in conjugated polymers. *Nat. Mater.* **12**, 1038–1044 (2013).
13. Podzorov, V. Conjugated polymers: long and winding polymeric roads. *Nat. Mater.* **12**, 947–948 (2013).
14. Glaudell, A. M., Cochran, J. E., Patel, S. N. & Chabinyc, M. L. Impact of the doping method on conductivity and thermopower in semiconducting polythiophenes. *Adv. Energy Mater.* **5**, 1401072 (2015).
15. Mott, N. F. & Davis, E. A. *Electronic Processes in Non-Crystalline Materials* 2nd edn (Oxford Univ. Press, 1979).
16. Overhof, H. & Thomas, P. in *Insulating and Semiconducting Glasses* (ed. Boolchand, P.) 553–606 (World Scientific, 2000).
17. Kaiser, A. B. Electronic transport properties of conducting polymers and carbon nanotubes. *Rep. Prog. Phys.* **64**, 1–49 (2001).
18. Bisquert, J. Interpretation of electron diffusion coefficient in organic and inorganic semiconductors with broad distributions of states. *Phys. Chem. Chem. Phys.* **10**, 3175–3194 (2008).
19. Shakouri, A. & Suqian, L. *Eighteenth International Conference on Thermoelectrics* 402–406 (IEEE, 1999).
20. Fistul, V. I. *Heavily Doped Semiconductors* Ch. 3 (Plenum Press, 1969).
21. Dohler, G. H. Conductivity, thermopower, and statistical shift in amorphous semiconductors. *Phys. Rev. B* **19**, 2083–2091 (1979).
22. Park, Y. W. Structure and morphology: relation to thermopower properties of conductive polymers. *Synth. Met.* **45**, 173–182 (1991).
23. Epstein, A. J. *et al.* Inhomogeneous disorder and the modified Drude metallic state of conducting polymers. *Synth. Met.* **65**, 149–157 (1994).
24. Wu, C.-G. & Chang, S.-S. Nanoscale measurements of conducting domains and current–voltage characteristics of chemically deposited polyaniline films. *J. Phys. Chem. B* **109**, 825–832 (2005).
25. Abeles, B., Pinch, H. L. & Gittleman, J. I. Percolation conductivity in W-Al<sub>2</sub>O<sub>3</sub> granular metal films. *Phys. Rev. Lett.* **35**, 247–250 (1975).
26. Kirkpatrick, S. Percolation and conduction. *Rev. Mod. Phys.* **45**, 574–588 (1973).
27. Duong, D. T. *et al.* Mechanism of crystallization and implications for charge transport in poly(3-ethylhexylthiophene) thin films. *Adv. Funct. Mater.* **24**, 4515–4521 (2014).
28. Kim, B., Shin, H., Park, T., Lim, H. & Kim, E. NIR-sensitive poly(3,4-ethylenedioxyxelenophene) derivatives for transparent photo-thermo-electric converters. *Adv. Mater.* **25**, 5483–5489 (2013).
29. Chang, W. B. *et al.* Electrochemical effects in thermoelectric polymers. *ACS Macro Lett.* **5**, 455–459 (2016).
30. Goldsmid, H. J. *Introduction to Thermoelectricity* Ch. 4 (Springer, 2010).
31. Lee, S. *et al.* Trap-limited and percolation conduction mechanisms in amorphous oxide semiconductor thin film transistors. *Appl. Phys. Lett.* **98**, 203508 (2011).
32. Grevin, B., Rannou, P., Payerne, R., Pron, A. & Travers, J. P. Scanning tunneling microscopy investigations of self-organized poly(3-hexylthiophene) two-dimensional polycrystals. *Adv. Mater.* **15**, 881–884 (2003).
33. Zhang, Q., Sun, Y., Xu, W. & Zhu, D. What to expect from conducting polymers on the playground of thermoelectricity: lessons learned from four high-mobility polymeric semiconductors. *Macromolecules* **47**, 609–615 (2014).
34. Sun, J. *et al.* Simultaneous increase in Seebeck coefficient and conductivity in a doped poly(alkylthiophene) blend with defined density of states. *Macromolecules* **43**, 2897–2903 (2010).
35. Xuan, Y. *et al.* Thermoelectric properties of conducting polymers: the case of poly(3-hexylthiophene). *Phys. Rev. B* **82**, 115454 (2010).

## Acknowledgements

The authors thank H. Katz, M. L. Chabinyc, A. M. Glaudell and H.-S. Kim for valuable discussions and O.-Y. Choi for assistance in figure illustration. This work was supported by the AFOSR MURI programme under FA9550-12-1-0002.

## Author contributions

S.D.K. developed the ideas and theory for this work. S.D.K. and G.J.S. prepared and edited the manuscript.

## Additional information

Supplementary information is available in the online version of the paper. Reprints and permissions information is available online at [www.nature.com/reprints](http://www.nature.com/reprints). Correspondence and requests for materials should be addressed to G.J.S.

## Competing financial interests

The authors declare no competing financial interests.

## Methods

**Model derivation.** The Boltzmann transport equations<sup>15,20</sup> can be described by using a transport function  $\sigma_E(E)$ . The conductivity and Seebeck coefficient can then be calculated using equations (1) and (3), respectively. Here we use the Fermi–Dirac distribution function:

$$f = \frac{1}{1 + e^{\frac{E - E_F}{k_B T}}} \quad (6)$$

which implies non-interacting fermions.

With the form of the transport function  $\sigma_E(E)$  given in equation (2), expressions for the transport properties can be simplified. Integrating by parts, equations (1) and (3) simplify to:

$$\sigma = \sigma_{E_0}(T) \times sF_{s-1}(\eta) \quad (7)$$

and

$$S = \frac{k_B}{e} \left[ \frac{(s+1)F_s(\eta)}{sF_{s-1}(\eta)} - \eta \right] \quad (8)$$

respectively. Here,  $F_i$  is the (non-normalized) complete Fermi–Dirac integral:

$$F_i(\eta) = \int_0^\infty \frac{e^i}{1 + e^{e-\eta}} d\epsilon \quad (9)$$

and  $e$  is the charge of the carrier (positive for p-type carriers).

It is seen that, for a given  $s$  parameter, thermopower is a function of only the reduced chemical potential  $\eta$ . Conductivity is directly proportional to the transport coefficient  $\sigma_{E_0}$ , while also depending on  $\eta$ . Each point on the  $S - \sigma$  curve (for example, Fig. 1c) corresponds to a particular  $\eta$ .